Surface Science 258 (1991) 23–34
North-Holland

surface science

Adsorption and reaction on oxide surfaces: NO, NO_2 on $Cr_2O_3(111)/Cr(110)$

C. Xu, M. Hassel, H. Kuhlenbeck and H.-J. Freund
Lehrstuhl für Physikalische Chemie I, Ruhr-Universität Bochum, Universitätsstrasse 150, D-4630 Bochum 1, Germany

Received 18 March 1991; accepted for publication 30 April 1991

We report results of electron spectroscopic measurements, i.e., LEED, EELS, ARUPS, XPS, and NEXAFS on NO, and NO_2 adsorbed on a thin Cr_2O_3 film with (111) orientation grown on top of a Cr(110) single-crystal surface via an oxidation procedure. It is shown that the $Cr_2O_3(111)$ surface is likely to consist of Cr-terminated and O-terminated terraces and that the Cr-atoms located within the oxide surface are in oxidation states different from the bulk. Our results indicate that these sites are involved in the dissociation of NO_2 at rather low temperature to yield adsorbed NO and adsorbed oxygen.

1. Introduction

Reports on surface science studies on adsorption on oxide surfaces have been rather scarce. This is particularly true for thin ordered oxide overlayers on metallic substrates [1]. To be able to apply the standard electron spectroscopic techniques of surface science we have chosen such substrates for our adsorbate studies.

Recently we have reported on adsorption of NO on a NiO(100) film, whose structure had been determined via LEED and STM. One interesting finding was that out of a group of four molecules NO, CO, NO_2 and CO_2 only NO would adsorb onto the surface. We were able to explain this behaviour on the basis of cluster calulations [2–4].

In the present study we report on the adsorption and reaction of NO and NO_2 with a $Cr_2O_3(111)$ surface grown on top of a Cr(110) single-crystal surface. We show mainly via EELS that this surface contains Cr atoms with oxidation states (close to Cr^{2+}) different from bulk Cr_2O_3 (close to Cr^{3+}). It appears that these states are primarily involved in the low-temperature dissociation of NO_2 observed on these surface. The dissociation product NO is detected on the surface.

2. Experimental

The experiments were performed in four ultrahigh vacuum systems. All systems contain facilities for LEED, AES and residual gas analysis with a quadrupole mass spectrometer. The EEL-spectra were recorded with a resolution of 200 meV for electronic excitation and 20 meV for vibration. ARUPS- and NEXAFS measurements were carried out with double-axis goniometers carrying electron energy analysers rotatable in two orthogonal planes with electron acceptance angles of 2° using light from the TGM-2 and HETGM-2 beamlines at the BESSY synchrotron radiation center in Berlin. The resolution was typically 100 meV. The XPS measurements were carried out on a modified Leybold XPS system equipped with a EA11 analyser and multi-channel detection. Radiation from a standard X-ray source with Al Kα anode is monochromatized using a 0.5 m Rowland set up. The base pressure in all system was below 2×10^{-10} Torr.

The Cr_2O_3 oxide films were grown according to the well-known procedure described in refs. [5–7] on a Cr(110) single-crystal substrate, prepared and cleaned by prolonged sputtering at $T = 800$ °C, until it displayed a contaminant free, well-ordered (1×1) surface. There is general

agreement that the oxide film is a well-ordered, (111)-oriented oxide surface [5,6,8]. After outgassing by flashing the crystal to 800 °C and subsequent cooling to 105 K the surface was exposed to NO and NO_2, respectively.

3. Results and discussion

3.1. The $Cr_2O_3(111)/Cr(110)$ surface

Fig. 1 shows a LEED pattern of the thin oxide film, which exhibits a hexagonal mesh with a lattice constant of 2.88 Å. The spots are more diffuse than the substrate spots, indicating a noticeable defect density in the oxide surface. However, as is clearly revealed by the LEED pattern, higher-order spots are very well visible indicating that there is long-range order within this oxide layer. The formation of such an oxide layer, together with its LEED pattern has been reported before and the earlier results are in perfect agreement with our findings [6,7]. Previous workers had already assumed that the structure of the surface is very similar to a bulk-terminated $Cr_2O_3(111)$ surface [5,6,8]. Of course, the (111)-surface may either be oxygen- or chromium-terminated as is obvious from fig. 2a, where a projection of the bulk Cr_2O_3 crystal structure as determined via X-ray crystallography [6,7] onto a plane containing the crystallographic c-axis is shown. The oxygen positions as well as the chromium positions are shown. An oxygen-terminated surface, as viewed along the c-axis, is shown in fig. 2b, and a chromium-terminated surface viewed along the same axis is shown in fig. 2c. Note that the given structures are bulk terminated structures which means that at the surface one expects two different, i.e., chemically inequivalent Cr sites marked as Cr_1 and Cr_2 in fig. 2a. These two chromium atoms only become inequivalent via the presence of the surface. Within the bulk all Cr atoms are equivalent and sit within a distorted octahedron or antiprism where one triangle of oxygen atoms is larger than the other one. This may also be recognized in fig. 2b, where the oxygen-terminated surface consists of small and large oxygen triangles. The thickness of the Cr_2O_3 layer may be estimated from the photoelectron spectra. Fig. 3a shows a set of angle-resolved photoelectron spectra for the flashed Cr_2O_3 surface. The peaks have been assigned

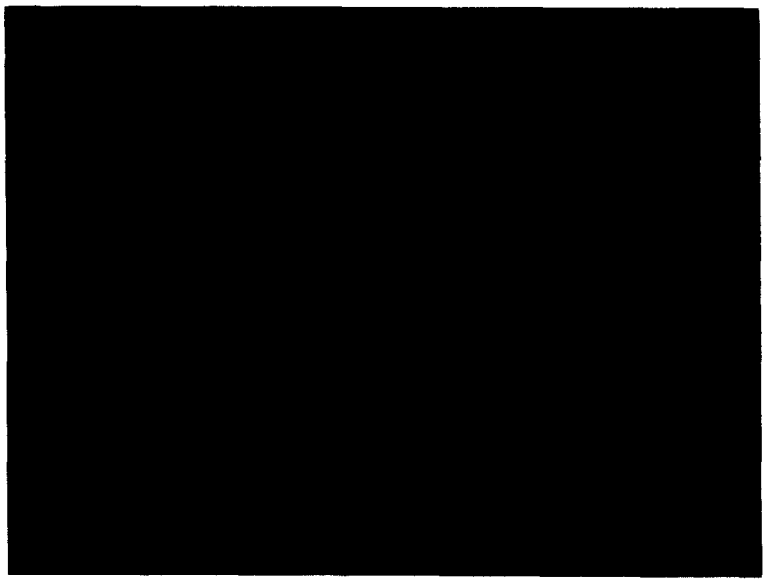

Fig. 1. LEED pattern of the hexagonal $Cr_2O_3(111)$ layer on Cr(110).

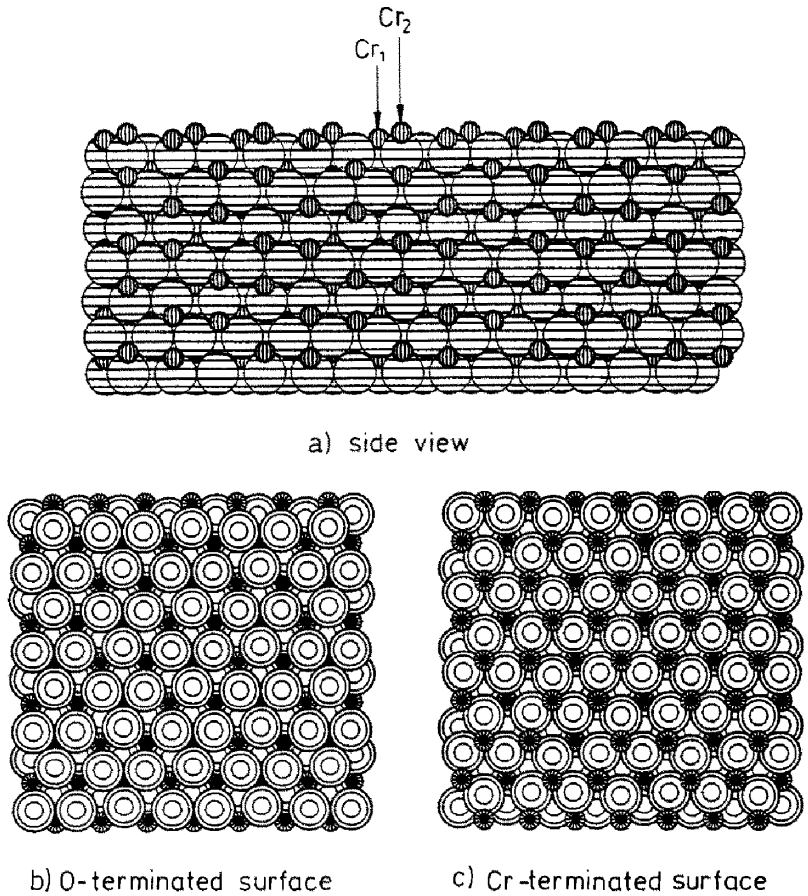

Fig. 2. Schematic representations of bulk Cr_2O_3 terminated by a (111) surface. (a) Side view. (b) Top view of the oxygen-terminated surface. (c) Top view of the chromium-terminated surface.

earlier for the clean surface [9,10]. Briefly, Cr^{3+} represents a d^3-system, with one occupied d-band which resides at lowest binding energy, about 3 eV below the Fermi level. The film must have a thickness of more than 2–4 layers otherwise emission from the Cr(110) substrate would be visible at the Fermi level. The relatively broad features at binding energies between 5 and 10 eV are due to oxygen induced bands.

As the photon energy is changed, angular momentum perpendicular to the surface varies. The observed dispersion as derived from the experimental data in fig. 3a is plotted in fig. 3b. It is indicative of the thickness of the Cr_2O_3 film and exhibits a well developed bandstructure perpendicular to the surface. At the present time it is not possible to compare the measured dispersion either to experimental dispersion data of the bulk crystal or to theoretical band structure calculations.

However, one may compare the experimental data which have been plotted in fig. 3b with the assumption of an inner potential of 8.5 eV – very simular to the one determined earlier for NiO – [3], to the result of a band structure calculation for an isomorphic oxide, i.e., Al_2O_3 [11]. Clearly, the electronic structures of Al_2O_3 and Cr_2O_3 are not identical. In particular, Cr_2O_3 contains d-electrons. The electronic structure of the oxygen sublattices however, should be comparable as far as band symmetries and relative bandwidths are concerned because all bands originate from O 2p

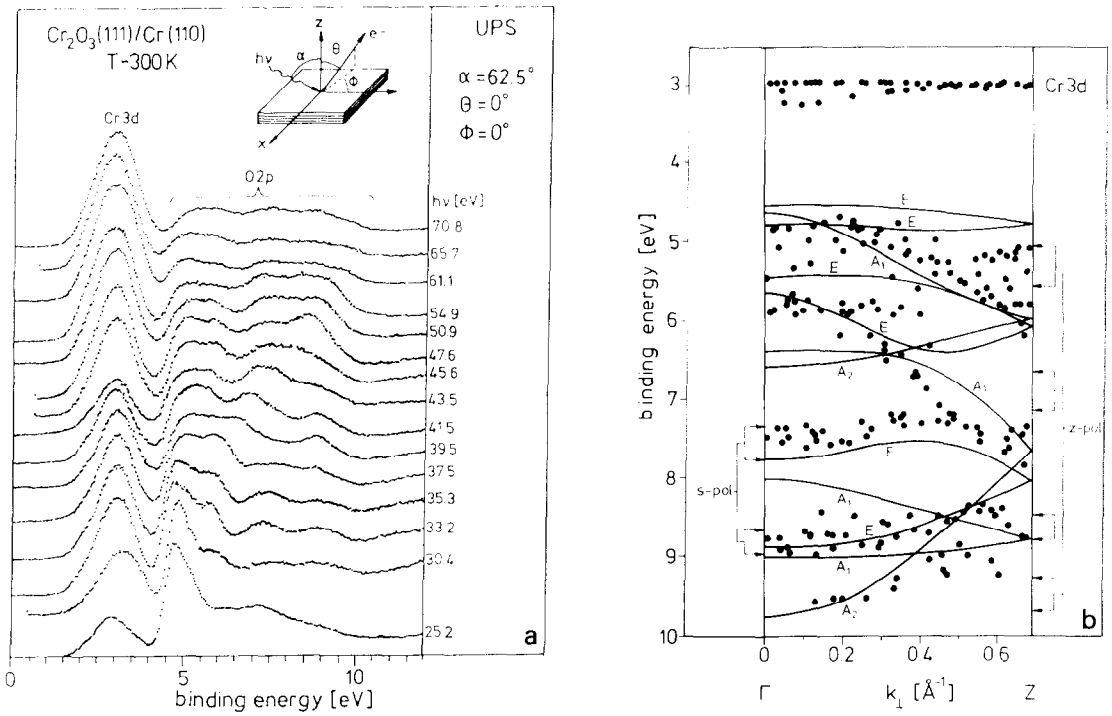

Fig. 3. ARUPS data for flashed $Cr_2O_3(111)/Cr(110)$ taken at normal electron emission. (a) Electron distribution curves for different photon energies. The binding energies are given relative to the Fermi level of the substrate. (b) E_B versus k dispersion plot as derived from the data shown in fig. 3a. The solid line is a calculated band structure of Al_2O_3 along the ΓZ direction [11] (see text). Those regions of the spectra that are most intense with s-polarized light are marked on left, and those which are most intense with predominantly z-polarized light are marked on the right hand side of the plot.

orbitals in first order. The overall absolute band widths on the other hand is expected to be different in Cr_2O_3 due to smaller O–O distances in Al_2O_3 and due to metal–O hybridization in Cr_2O_3. We have tried to take this into account by scaling the bandwidth of the calculated band structure so as to achieve the best fit with our experimental data. The comparison is shown in fig. 3b.

Al_2O_3 has six oxygen atoms within its unit cell leading to 18 O 2p atomic wavefunctions which have to be combined so as to form Al_2O_3 bands. Along the ΓZ direction, which is the direction perpendicular to the surface, we have C_{3v} symmetry. From the symmetries which label the bands we may qualitatively deduce the polarization dependence of the photoemission features assuming that the correlation of the Al_2O_3 band structure with our measured Cr_2O_3 dispersion is significant. Four O $2p_z$ derived bands are of A_1 symmetry and suggest strong emission with z-polarized light. This is in line with the observation that the two band systems dispersing between 5 and 6 eV, and between 6 and 7.5 eV, as well as the feature around 9.5 eV binding energy are prominent with z-polarization. On the other hand, the bands with the relatively small dispersion are most intense when excited with s-polarized light. It is therefore fair to state that at least some features of the band structure can be found in the experimental data, justifying a posteriori the comparison made. The band at 3 eV binding energy is due to ionization of the Cr 3d-derived band. Due to the strong localization of the 3d electrons the dispersion is very small. At particular energies where the 3d bands show pronounced resonances we observe an apparent dispersion which, however, is not correlated with the size of the Brillouin zone. We believe that the energy stabilization near Γ is due to the action of the photovoltaic effect as dis-

cussed by Horn [12]. Another explanation might involve the antiferromagnetic properties of Cr_2O_3 but we have no further indications supporting the latter hypotheses.

The problem that has to be faced next is the question which termination, either oxygen or chromium, actually is present on our sample surfaces.

The ELS results which are discussed in the following imply that at least part of the surface exhibits Cr ions with a different charge than the bulk ions. Fig. 4a shows a set of ELS spectra recorded with a primary electron energy of 100 eV over a wide range of loss energies.

In the inset in fig. 4a we show a comparison between the imaginary part of the bulk dielectric functions of Cr_2O_3 and Al_2O_3 [13,14] and the loss function observed for our Cr_2O_3 film. Al_2O_3 has been incluced to identify excitations not involving d-electrons but rather cation-bound excitons and interband transitions within the oxygen-derived band system. This comparison is possible because Al_2O_3 and Cr_2O_3 are isomorphic, as pointed out above, but have slightly different lattice constants. The comparison suggests that the features below 8–9 eV are connected with excitations from or into the partly occupied d-levels of the chromium ions. McClure [15] has estimated that the minimal energy nessesary to excite a ligand to metal (i.e., $O \rightarrow Cr$) charge transfer transition is 6.2 eV, indicating that the transitions below 5 eV shown on an enlarged scale in fig. 4b are caused by d–d transitions. According to the literature [16] the broad features at 7.5 and 9.9 eV should be assigned to charge-transfer transitions of the type discussed above, where the oxygen–chromium joint density of states (see fig. 2) shows up. While there is little

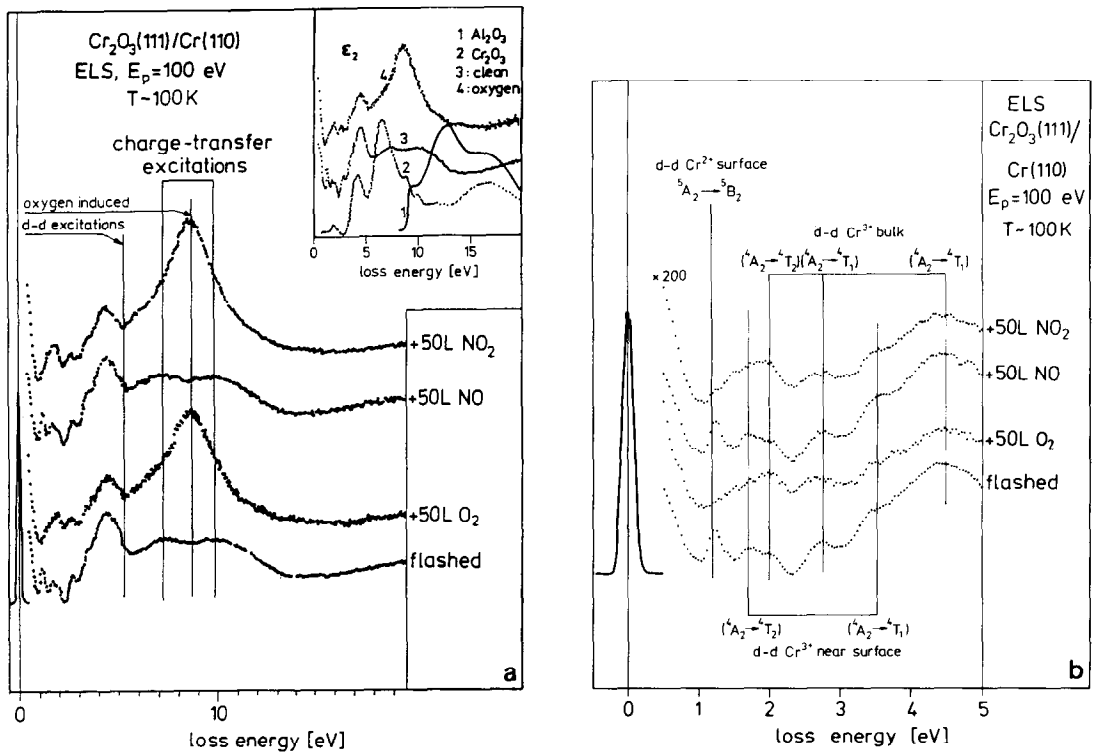

Fig. 4. Electron energy loss spectra in the electronic regime for $Cr_2O_3(111)/Cr(110)$ before and after exposure to various gases. (a) Wide scan plot. The inset shows a comparison between the bulk dielectric functions of Al_2O_3 [13] (1) and Cr_2O_3 [14] (2) with the loss spectra of $Cr_2O_3(111)$, flashed (3) and after O_2 exposure (4). (b) Expanded view of the loss region of fig. 4a with an assignment of the spectral features (see text).

doubt about this assignment for the second of the two broad features, the Al_2O_3 data suggest that in this region interband transitions begin to play a role.

In order to attempt a detailed assignment we start with fig. 4b. The energy region shown in fig. 4b provides the clue for the discussion of the electronic structure of the Cr-ions within the surface region. It is known from the literature that there are three d–d transitions allowed for a Cr d^3-configuration in the quasi-octahedral (antiprismatic) environment of the Cr_2O_3 bulk compound [17–20]. The ground state of the Cr ion is a $^4A_2$ state. Within the considered energy range there are three ^4A states available. These ^4A-states are split off from the two $^4T_1(^4A_2)$ states and one $^4T_2(^4A_1)$ state of an octahedrally symmetric $(Cr^{3+}O_6^{12-})$ moiety due to the reduced symmetry. The energy of the latter states relative to the presented state can be estimated from the well known Tanabe–Sugano diagrams, if we assume a rather small energy splitting due to symmetry breaking [17,18]. It may be safely assumed, on the basis of such an estimate, that the transition energies are close to those observed for bulk Cr_2O_3 [16] or Cr^{3+} embedded in Al_2O_3 [18]. There are three transitions at 2.08, 2.83 and 4.9 eV for the latter system which are marked in fig. 4b as d–d-Cr^{3+} bulk transitions. For the first two transitions the observed intensities are compatible with the assignment as d–d-transitions. The third transition, however, at 4.9 eV exhibits an intensity that is too high to be exclusively due to a d–d transition on a single Cr^{3+}-ion. Even though it is known that via Cr–Cr interactions, e.g., in Cr_2O_3, the relative intensity of the transition grows considerably [21–23], this intensity increase is not high enough to explain the observed intensity of the 5 eV loss feature. Whether there is a collective excitation within the Cr-sublattice responsible for the high intensity cannot be decided at this time.

In our further discussion of the loss features we have to consider the limited escape depth of the incident electrons. Electrons of 100 eV kinetic energy probe a depth of 5 Å, i.e., the scattered electrons carry information from the first four layers, i.e., two oxygen and two chromium layers. We believe that the second chromium layer of an oxygen-terminated surface already represents the bulk situation, and that it is this and the following layers that gives rise to the signals discussed above. The first chromium layer of an oxygen terminated surface, however, should be chemically different from the bulk-like layers. We assign the features marked "near surface" to excitations involving d–d transitions within the first layer. Another possible origin of the features may be spin-flip transitions [19] but we feel that the observed intensities are too large considering 100 eV primary energy where intensities are likely to be governed by dipole selection rules.

We now turn to the Cr-terminated patches of the surface. If we keep the Racah parameter for the oxygen ligand fields as in the bulk and reduce the number of oxygen atoms coordinated to the Cr ion, the separation between the ground state and the first allowed excited state is expected to be considerably smaller than the separation between ground and first dipole allowed excited state in the octahedral case, because there are only three nearest-neighbour oxygen atoms (fig. 2). Concomitantly it is likely that it is more favourable for the chromium to reduce its charge state from 3+ to 2+. A detailed analysis and comparison with Cr^{2+} excitation spectra in molecular complexes [20] shows that Cr^{2+} is characterized by a single low-lying dipole allowed transition, in agreement with the sharp single loss feature found in fig. 4b. Also, Cr ions in any other d-electron configuration, except the d^1-configuration of Cr^{5+}, which is unrealistic, would lead to more than one well separated allowed transition. Sofar the analysis has led us to the conclusion that the pronounced loss feature at about 1.6 eV loss energy must be due to chromium ions located at the oxide surface and carrying a lower charge (2+) than the bulk chromium ions (3+).

The proof for the localization of the 1.2 eV feature in the surface region, however, is drawn from oxygen adsorption experiments. If we expose the oxide surface to molecular oxygen at low temperature (110 K, fig. 4b) the peak at 1.2 eV disappears, and a relatively broad, very intense

feature just below 10 eV loss energy shows up. We interpret this finding as an indication for oxygen dissociation. The oxygen atoms coordinate the Cr^{2+} ions, which in the process are oxidized towards C^{3+} ions. The newly adsorbed oxygen atoms will then of course contribute to the excitation spectra in such a way that the intensity of the transitions within the oxygen sublattice increases as observed. It is not clear at present how the adsorbed atomic oxygen is coordinated towards the Cr ions, however the appearance of the intense band at 10 eV which we associate with adsorbed oxygen indicates that the coordination is not identical to the situation at those parts of the surface which are oxygen terminated.

The results of the EELS studies are basically corroborated by XP-spectra of the $Cr\,2p_{3/2}$ states of the system. Fig. 5 shows a set of spectra with the one of the flashed oxide surface at the bottom. There are two dominant features at 576.0 and 577.0 eV binding energy which we assign to Cr^{2+} and Cr^{3+} ionizations, respectively. The small peak at 574.2 eV binding energy which is due to metallic Cr (see the $Cr\,2p_{3/2}$ spectrum of a clean Cr(110) surface for comparison) is strongly attenutated due to the presence of the oxide film. The observed difference in binding energies is compatible with observed chemical shifts of chromium ions in chemical environments equivalent to Cr^{2+} and Cr^{3+}, e.g, CrF_2 and CrF_3 [24]. The Cr^{2+} intensity is attenuated when the surface is exposed to oxygen from the gas phase, clearly indicating that at least part of the Cr^{2+} ions are located in the surface region as suggested by the more surface sensitive EELS measurements. The observed shift of the Cr 2p ionizations with respect to the metal ionizations of the oxide film before and after oxygen exposure is interesting and shall be discussed in detail elsewhere. The intensity remaining in the region of the Cr^{2+} ionizations could be due to Cr^{2+} which may be located in the neighborhood of the metal–oxide interface.

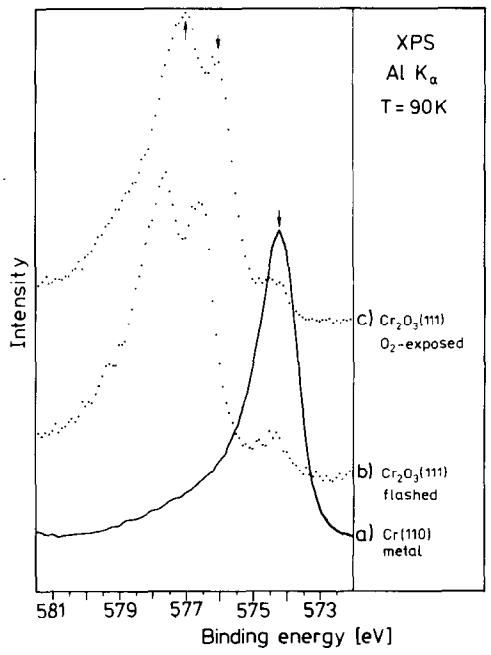

Fig. 5. $Cr\,2p_{3/2}$ XP-spectra of a clean Cr(110) surface (a), a flashed, grown Cr_2O_3(111) film (b), and a Cr_2O_3(111) film exposed to oxygen (c).

Summarizing sofar, there is evidence that at the Cr_2O_3 surface there exist Cr ions in a lower oxidation state than Cr^{3+} which may react with dosed molecular oxygen and are oxidized by dissociating oxygen molecules.

3.2. Adsorption of NO

As judged by TDS the desorption maximum for NO on Cr_2O_3(111) is at 340 K Thus NO is chemisorbed on chromium oxide. We have studied the adsorption of NO with HREEL-spectroscopy in the vibronic regime. Fig. 6 shows at the bottom the spectrum of clean Cr_2O_3 (a) taken with 10 eV primary electron energy. It is a typical oxide vibronic loss spectrum exhibiting very intense Fuchs–Kliewer phonons [25]. Spectrum (b) is a trace of the NO-covered surface and it exhibits the NO loss at 1791 cm^{-1} which is typical for NO adsorbed on top of a metal ion within an oxide surface as we have demonstrated recently for the case of NO/NiO(100) [2,3,26]. In addition to the NO loss we observe a feature at 2480 cm^{-1}. We assign this feature to a combination band, i.e., a Fuchs–Kliewer phonon of the surface at 700 cm^{-1} and the NO stretch. Similar to the case of NO adsorption on NiO the NO stretching vibration is the only loss we are able to

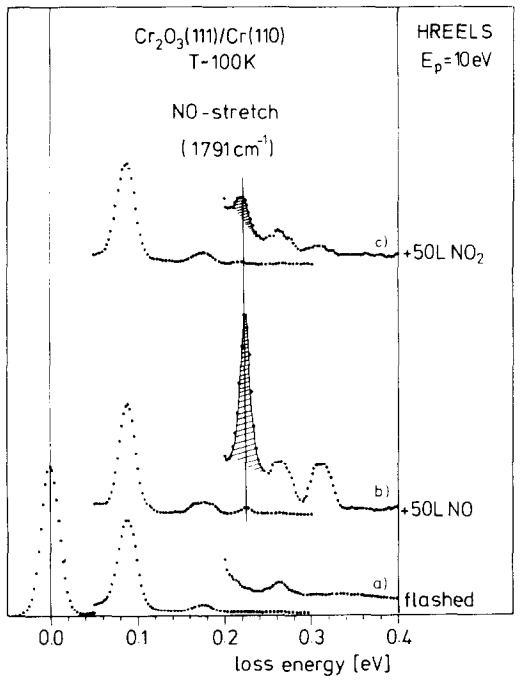

Fig. 6. Electron energy loss spectra in the vibronic regime before (flashed) and after exposure to NO and NO_2, respectively.

identify because the very strong Fuchs–Kliewer-phonons cover up the region of metal molecule vibrations and bending modes. It appears therefore hard at this point to extract information about the bonding geometry of NO on the Cr_2O_3(111) surface purely on the basis of EELS-spectra.

We have therefore employed ARUPS and NEXAFS to achieve a deeper insight into this problem. Fig. 7a shows two sets of angle-resolved photoelectron spectra of NO on Cr_2O_3(111) where the electrons have been collected in the so-called allowed and forbidden geometries [27,28]. In the allowed geometry the electrons are detected within the plane spanned by the direction of light propagation and light polarization (incidence plane). Ion states of σ symmetry of molecules with their axis oriented perpendicularly to the surface show up in this geometry, while those states do not emit into a plane perpendicular to the incidence plane (forbidden geometry). If the molecular axis is bent with respect to the surface normal the intensities of σ ion states vary between the electron detection geometries depending on the tilt of the molecular axis. Fig. 7a shows two NO-induced features in the spectrum taken in allowed geometry. These peaks are due to ionization of the $5\sigma/1\pi$ and 4σ ion states of adsorbed NO as may be assigned on the basis of ARUP-spectra reported for NO adsorbates on metal surfaces in the literature [26,28]. From a comparison of allowed and forbidden geometries it is found, that the σ ion state intensities are considerably higher in the former collection geometry. However, the 4σ intensity, for example, is not fully attenuated in the forbidden geometry. Even if we take the incomplete polarization of the synchrotron light into account the remaining intensity of the 4σ ion state in the forbidden geometry can only be explained by a non vertical adsorption geometry of NO. It is, however, very difficult to quantitatively estimate the tilt angle from the data in fig. 7a. Therefore we show in fig. 7b a series of ARUP-spectra where the angle between the direction of the incident radiation and the direction of the emitted electrons has been kept constant, while the angle of incidence (α) with respect to the surface normal has been varied. It is obvious that the 4σ ion state intensity assumes a maximum value at about $\alpha = 60°$. At $\alpha = 60°$ the polarization vector is at an angle of 30° with respect to the surface normal. Since the 4σ ion-state intensity should be maximal when the direction of the polarization vector coincides with the molecular axis we may estimate a tilt angle of about 30° for NO on Cr_2O_3(111) with respect to the surface normal. In this discussion the damping of the light at the surface according to the Fresnel formulae has been neglected since the optical constants for this thin oxide film on Cr(110) are not known. Thus the derived tilting angle is only correct within at least $\pm 10°$.

A qualitatively similar result follows from the analysis of the NEXAFS data as shown below. Fig. 8a shows a set of NEXAFS spectra taken at the nitrogen K-edge. Spectrum (a) shows the features (satellite and O2s photoemission) due to the clean metal oxide surface. Spectrum (b) is taken from the NO-covered surface. There are

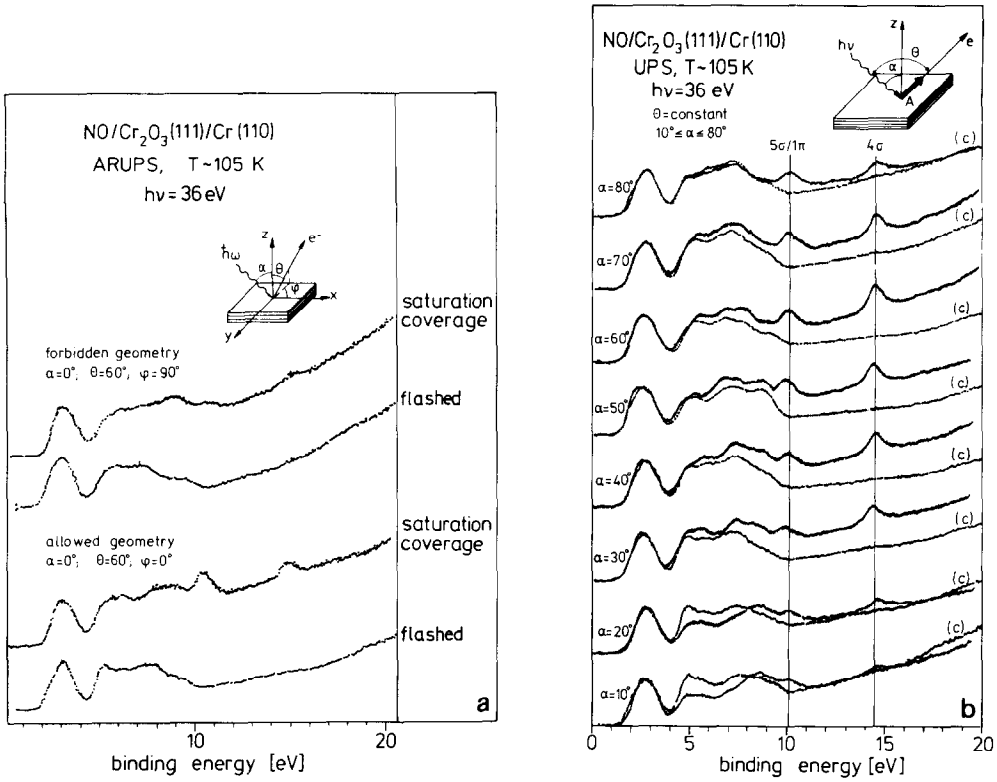

Fig. 7. ARUP spectra of flashed $Cr_2O_3(111)$ and $Cr_2O_3(111)$ exposed to NO. (a) Spectra taken in the "allowed" and the "forbidden" geometry. (b) Series of spectra taken with a constant angle between the direction of the incident light and the electron emission direction. The light incidence angle with respect to the surface normal is varied. For each light incidence angle the spectra of the flashed (c) and the NO covered surface are shown.

basically two adsorbate induced features in the spectrum that are of interest to the present question. The feature with the smaller line width and lower photon energy is the so-called π resonance, the one at higher photon energy with large line width in the so-called σ-shape resonance. For a molecule with perpendicular orientation with respect to the surface plane one expects an increase of the relative intensity of the σ-shape resonance with respect to the π-resonance for small incident angles according to the curve plotted in fig. 8b. Clearly the observed intensity variations (fig. 8b) are not typical for a molecule with vertical orientation. The data points derived from the present experimental data, shown in fig. 8b can be fit best by a curve for which an angle of 50° between the molecular axis and the surface normal has been assumed [29,30]. This is slighly different from the value deduced from ARUPS data. Since we could not correct the light polarization at the surface according to the Fresnel formulae and since the determination of the σ-shape resonance intensities was rather problematic there are considerable error bars on these NEXAFS results. Therefore, the present data are only taken qualitatively and lead to the conclusion that NO is adsorbed on top of a metal ion in a bent configuration.

The bonding of NO towards the oxide surface may be judged via two experimental observations. Firstly, the vibrational stretching frequency as observed via HREELS (fig. 6) indicates on-top metal ion adsorption as discussed above. Secondly, the adsorption of NO has little effect on the electronic transitions as observed by ELS (fig. 4b). The spectra of the clean and the NO

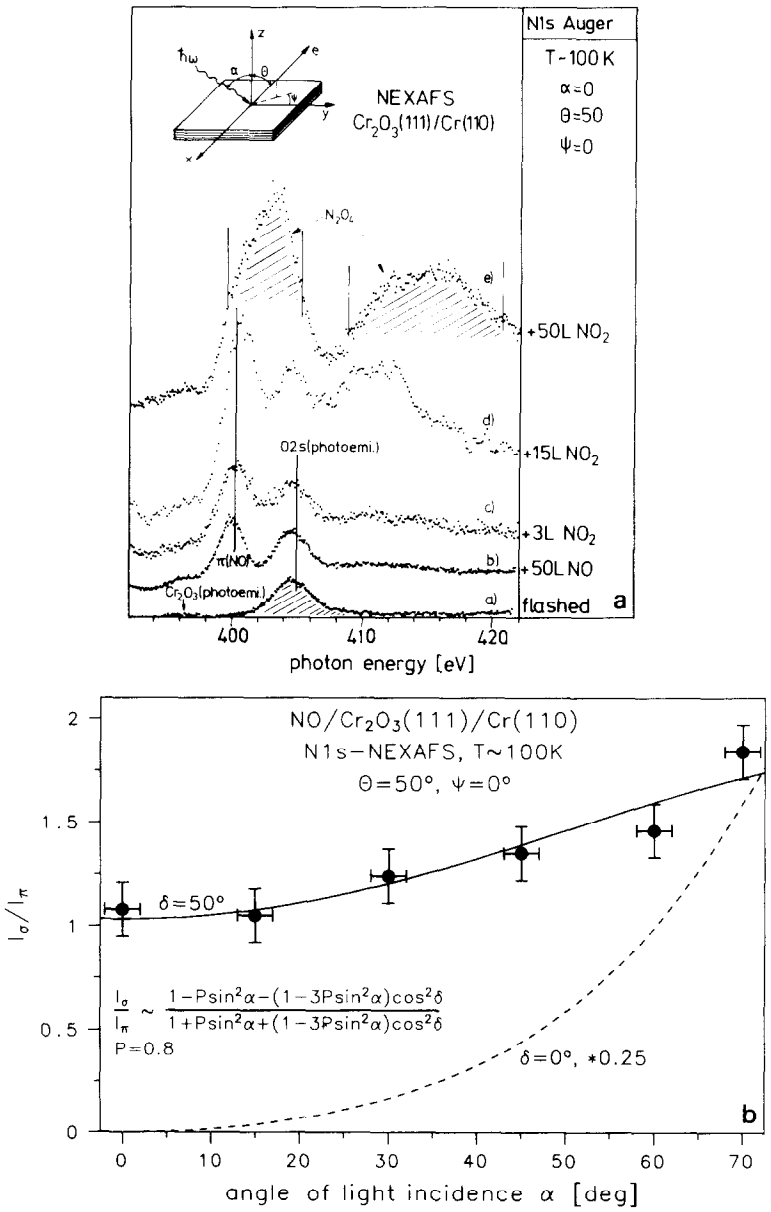

Fig. 8. NEXAFS data for clean and adsorbate covered $Cr_2O_3(111)/Cr(110)$. (a) NEXAFS spectra of the flashed $Cr_2O_3(111)$ surface and $Cr_2O_3(111)$ exposed to NO and increasing amounts of NO_2, respectively. (b) Ratio of the intensities of the N 1s $\rightarrow \pi$ resonance and the N 1s $\rightarrow \sigma$ resonance as a function of the light incidence angle α for NO on $Cr_2O_3(111)$. Calculated curves are shown for a tilt angle of $\delta = 50°$ and for NO standing upright on the surface.

covered surface are very similar, except for a noticeable decrease of the Cr^{2+} d–d loss intensity relative the Cr^{3+} d–d transitions. This indicates in our opinion that these states are involved in the bonding.

2.3. Adsorption of NO_2

In the case of NO_2 adsorption the situation at the surface is more complicated as compared with NO adsorption. While the ARUPS data (not

shown here) are inconclusive, the EELS data of fig. 6, spectrum (c), show no evidence for the presence of NO_2 on the surface at low NO_2 exposures even at low temperatures. However, as is obvious by comparison with the data on pure NO adsorption, spectrum (c) reveals the presence of NO on the oxide surface after NO_2 exposure. The NO vibrational frequency is very similar to the one observed for pure NO adsorption. We must therefore conclude that the NO bonding site after NO_2 exposure is the same as after pure NO exposure. Upon inspection of the NO_2 NEXAFS data in fig. 8a we observe upon comparison with the data for NO in the same figure that this conclusion is strongly supported. Additional support in supplied by TD-spectra (not shown here) where a strong NO desorption signal is observed from the NO_2 dosed surface at the temperature where desorption occurs for the pure NO adsorbate. At higher doses of NO_2 we start to see NEXAFS signals due to the formation of N_2O_4 dimers, as shown at the top of fig. 8a. This conclusion may be drawn in comparison with NEXAFS data recently reported by Geisler et al. [31] on NO_2 absorption on Ni(100), where it was shown that an assignment of the spectral features may be given on the basis of excitation of the N 1s electron into molecular valence states of the N_2O_4 dimer.

Very interesting changes upon NO_2 adsorption are observed in the EEL-spectra in the electronic regime as revealed by inspection of figs. 4a and 4b. The Cr^{2+} d–d loss is attennuated upon NO_2 adsorption and in addition the strong, very broad loss close to 9 eV appears. The similarity of this finding with the results upon oxygen adsorption very strongly corroborates the interpretation given above that these changes are caused by adsorption of atomic oxygen. In the case of NO_2 the source for atomic oxygen is the NO_2 molecule itself which dissociates into NO and oxygen as suggested by the HREELS data.

Summarizing the last section so far, we find that when NO_2 is adsorbed onto a clean $Cr_2O_3(111)/Cr(110)$ surface it dissociates into oxygen and NO. We know from ELS that the NO and O remain on the surface. The remaining oxygen results in the strong loss feature in the ELS spectra close to 10 eV, and in a simultaneous attenuation of the Cr_2 + loss, similar to the situation observed after pure oxygen exposure. We believe, that the oxygen, which is released in the dissociation process leads to the oxidation of Cr^{2+} to Cr^{3+} and NO_2 is reduced to NO. We can follow the oxidation of the Cr^{2+} by looking at the disappearence of the 1.2 eV loss feature as has been pointed out above in connection with the exposure of the Cr_2O_3 oxide surface towards oxygen.

Acknowledgements

We are grateful to the Deutsche Forschungsgemeinschaft, the Bundesministerium für Forschung und Technologie and the Ministerium für Wissenschaft und Forschung des Landes NRW for funding our research.

HJF thanks the Fond der Chemischen Industrie for financial support.

References

[1] V.E. Henrich, Rep. Prog. Phys. 48 (1985) 1481.
[2] H. Kuhlenbeck, G. Odörfer, R. Jaeger, C. Xu, Th. Mull, B. Baumeister, G. Illing, M. Menges, H.-J. Freund, D. Weide, P. Andresen, G. Watson and E.W. Plummer, Vacuum 41 (1990) 34.
[3] H. Kuhlenbeck, G. Odörfer, R. Jaeger, G. Illing, M. Menges, Th. Mull, H.-J. Freund, M. Pöhlchen, V. Staemmler, S. Witzel, C. Scharfschwerdt, K. Wennemann, T. Liedtke and M. Neumann, Phys. Rev. B 43 (1991) 1969.
[4] M. Bäumer, D. Cappus, H. Kuhlenbeck, H.-J. Freund, G. Wilhelmi, A. Brodde and H. Neddermeyer, Surf. Sci. 253 (1991) 116.
[5] H.M. Kennett and A.E. Lee, Surf. Sci. 33 (1972) 377.
[6] P. Michel and C. Jardin, Surf. Sci. 36 (1973) 478.
[7] S. Ekelund and C. Leygraf, Surf. Sci. 40 (1973) 179.
[8] F. Watari and J.M. Cowley, Surf. Sci. 105 (1981) 240.
[9] G.K. Wertheim, H.J. Guggenheim and S. Hüfner, Phys. Rev. Lett. 30 (1973) 1050.
[10] D.E. Eastman and J.L. Freeouf, Phys. Rev. Lett. 34 (1975) 395.
[11] I.P. Batra, J. Phys. C (Solid State Phys.) 15 (1982) 5399.
[12] K. Horn, Appl. Phys. A 51 (1990) 389.
[13] E.T. Arakawa and M.W. Williams, J. Phys. Chem. Solids 29 (1968) 735.

[14] T.I.Y. Allos, R.R. Birss, M.R. Parker, E. Ellis and D.W. Johnson, Solid State Commun. 24 (1977) 129.
[15] D.S. McClure, Electronic States of Inorganic Compounds: Experimental Techniques, Ed. P. Day (Reidel, Dordrecht, 1975) pp. 113–139.
[16] Y. Sakisaka, H. Kato and M. Onchi, Surf. Sci. 120 (1982) 150.
[17] D.S. McClure, Solid State Phys. 9 (1959) 399.
[18] D.S. McClure, J. Chem. Phys. 38 (1963) 2289.
[19] K.W. Blazey, Solid State Commun. 11 (1972) 371.
[20] S. Sugano, Y. Tanabe and H. Kamimura, Multiplets of Transition Metal Ions in Crystals (Academic Press, New York, 1970).
[21] G. Smith, Phys. Chem. Minerals 3 (1978) 375.
[22] G. Amthauer and G.R. Rossman, Phys. Chem. Minerals, 11 (1984) 37.
[23] S.M. Mattson and G.R. Rossman, Phys. Chem. Minerals 14 (1987) 163.
[24] R. Merryfield, M. McDaniel and G. Parks, J. Catal. 77 (1982) 348.
[25] K.L. Kliewer and R. Fuchs, Adv. Chem. Phys. 27 (1974) 335.
[26] G. Odörfer, R. Jaeger, G. Illing, H. Kuhlenbeck and H.-J. Freund, Surf. Sci. 332 (1990) 44.
[27] E.W. Plummer and W. Eberhardt, Adv. Chem. Phys. 49 (1982) 533.
[28] H.-J. Freund and M. Neumann, Appl. Phys. A 47 (1988) 3.
[29] J. Somers, M.E. Kordesch, Th. Lindner, H. Conrad, A.M. Bradshaw and G.P. Williams, Surf. Sci. 188 (1987) L693.
[30] J. Stöhr and D.A. Outka, Phys. Rev. B 36 (1987) 7891.
[31] H. Geisler, G. Odörfer, G. Illing, R. Jaeger, H.-J. Freund, G. Watson, E.W. Plummer, M. Neuber and M. Neumann, Surf. Sci. 234 (1990) 237.